For the data of Fig. 2 and a crystal $l = 0.3$ cm thick the reflecting layer is $l_0 \gtrsim 0.05$ cm thick.

The large difference between the transient currents obtained under reflection conditions during the first and subsequent exposures can be explained in a similar manner. We must simply allow for the fact that after the end of illumination the grating of ϵ^1 remains because of the faster relaxation of the conductivity of the crystal.

We shall conclude by pointing out that the strong dependence of the nonlinear interaction of waves on the polar axis orientation is not specific to the problem under discussion. Such a dependence exists, for example, in the interaction of two waves incident on the surface of a crystal parallel to the optic axis.[2-3] A common feature in such problems is the amplification of waves with a negative projection of the wave vector on the polar axis. In the final analysis, this result is due to the phase shift between the recorded gratings, i.e., it is due to the quarter-period mismatch between the modulations of the intensity and refractive index.[8]

1)The direction of the c axis is determined by the fact that $E \parallel c$ alters the permittivity by an amount $\Delta \epsilon < 0$.
2)The zeroth harmonic ϵ^0 is excluded from the system (4) by the phase shift.
3)Initially the total reflection coefficient (calculated ignoring absorption) should be regarded as equal to 2β because the faces of a crystal may be slightly out of parallel.[7]

1D. I. Stasel'ko and V. G. Sidorovich, Zh. Tekh. Fiz. 44, 580 (1974) [Sov. Phys. Tech. Phys. 19, 361 (1974)].
2B. I. Sturman, Preprint No. 48 [in Russian], Institute of Automation and Electrometry, Siberian Branch of the Academy of Sciences of the USSR, Novosibirsk (1977); Zh. Tekh. Fiz. 48, 1010 (1978) [Sov. Phys. Tech. Phys. 23, (1978)].
3V. L. Vinetskiĭ, N. V. Kukhtarev, V. B. Markov, S. G. Odulov, and M. S. Soskin, Izv. Akad. Nauk SSSR Ser. Fiz. 41, 811 (1977).
4N. Bloembergen, Nonlinear Optics, Benjamin, New York, 1965 (Russ. Transl., Mir, M. 1966).
5A. M. Glass, D. von der Linde, and T. J. Negran, Appl. Phys. Lett. 25, 233 (1974); A. M. Glass, D. von der Linde, D. H. Auston, and T. J. Negran, J. Electron. Mater. 4, 915 (1975).
6V. I. Belinicher, V. K. Malinovskiĭ, and B. I. Sturman, Zh. Eksp. Teor. Fiz. 73, 692 (1977) [Sov. Phys. JETP 46, 362 (1977)].
7M. Born and E. Wolf, Principles of Optics, 3rd. ed., Pergamon Press, Oxford, 1965 (Russ. Transl., Nauka, M., 1970).
8J. J. Amodei, Appl. Phys. Lett. 18, 22 (1971).

Translated by A. Tybulewicz

Formation of He+ ions in various electronic states in He+2 + He collisions

V. V. Afrosimov, A. A. Basalaev, G. A. Leĭko, and M. N. Panov

A. F. Ioffe Physicotechnical Institute, USSR Academy of Sciences

One-electron capture ($He^{+2} + He \rightarrow He^+ + He^+$) and capture with ionization ($He^{+2} + He \rightarrow He^+ + He^{+2} + e^-$) in $He^{+2} + He$ collisions have been investigated for He^{+2} kinetic energies T_0 from 2 to 60 keV. To recognize the processes, both particles from a given collision were recorded by a coincidence technique. For the first time ever, the charge states of the particles were analyzed and the kinetic energy losses and scattering angle of the fast particle were measured for the same collisions. This made it possible to measure the cross sections for elementary processes involving changes in the charge states with the production of particles in definite electronic states and taking place at a fixed impact parameter. It is shown that in the capture process one of the He^+ ions is formed in an excited state with overwhelming probability (~75% at $T_0 = 60$ keV and nearly 100% at $T_0 = 2$ keV). The energy distributions of the electrons released in capture-with-ionization processes corresponding to definite impact parameters were determined. The impact-parameter dependence of the distributions shows that the capture-with-ionization process is a result of the decay of an autoionization state of the He_2^{+2} quasimolecule. The internuclear distances at which the inelastic transitions take place (as determined from the scattering of the fast He^+ ions) agree with those expected on the basis of the terms of the He_2^{+2} system. It is concluded that the quasimolecular model of the interaction of atomic particles can account well for the features of the $He^{+2} + He$ collision.

PACS numbers: 34.70.+e, 34.50.Hc

I. INTRODUCTION

The two-electron system $He^{+2} + He$ provides one of the simplest examples of the interaction of multiply charged ions with atoms and has been repeatedly investigated, both experimentally and theoretically. Most of the experimental studies, however, were not based on the direct investigation of the processes taking place in He^{+2} + He collisions, but on an analysis of the charge states of one of the particles (either the fast one or the slow

one) leaving the collision.[1,2] The authors of Refs. 3 also investigated the electronic states of the fast He⁺ ions formed as a result of electron capture by analyzing the kinetic energy change in the collision; it was noted that these ions are found in excited states.

In our earlier studies[4] we measured the cross sections for all the elementary processes involving change in the charge states of the particles in He^{2+} + He collisions, using a coincidence technique to register both the particles. We also obtained the first information on the distribution of the He⁺ ions produced in the one-electron capture process over their energy states.[5] Nevertheless, a considerably more detailed analysis of the processes taking place will be required in order to elucidate the interaction mechanism operative in the He^{+2} + He collisions under consideration—a very simple case of the collision of a multiply charged ion with an atom. Such an analysis would include determination of the populations of the electronic states of the produced ions, the absolute cross sections of the corresponding channels for each process, and the internuclear distances in the collision at which the electronic transitions take place.

II. EXPERIMENTAL SETUP AND MEASURING TECHNIQUE

In the apparatus (diagrammed in Fig. 1) a beam of He^{+2} ions, produced in the electron-impact ion source I and accelerated to the desired energy T_0, passed through the magnetic monochromator M and the collimating apertures CA_1–CA_3 and entered the target chamber TC containing the target gas. Before reaching the target chamber the beam was displaced parallel to itself by the electrostatic field produced by electrodes E_1 in order to eliminate particles that undergo charge exchange with residual gas atoms on the way to the chamber. The entrance aperture CA_3 to the target chamber measured 1×1 mm, while the primary beam had an angular spread of 3' and an energy spread of 0.8 eV.
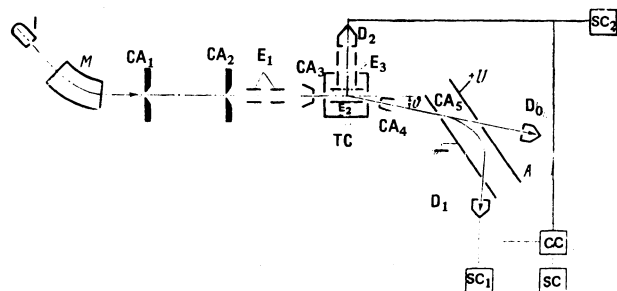
Fast particles that had been scattered through a spe-

cified angle θ by collisions in the target chamber were selected by a collimator (apertures CA_4 and CA_5) which could be rotated about the center of the target chamber. The instrumental angular-scattering contour was ~20' wide at the base. The fast particles were charge separated and kinetic-energy analyzed by the electrostatic analyzer A, which had plane electrodes, and were subsequently registered by detector D_1 and scaling circuit SC_1. The energy resolving power of the entire setup amounted to ~4000 at half height of the instrumental contour.

The slow ions produced in the target gas were extracted from the chamber, toward the side of the beam opposite that toward which the fast particles were scattered, by the electric field between the electrodes E_2. This made it possible, while using low electric field strengths (~5 V/cm) between the electrodes E_2, to obtain a full collection of slow ions that were collision partners of the recorded fast particles. It is important to use a weak field in order not adversely to affect the angular resolution in measuring the differential cross section for scattering of the fast particles. Then the slow ions passed through a 15×20 mm window in one of the electrodes E_2, which was covered by a screen of transparency 95%, and entered the strong electric field of the electrodes E_3, which accelerated and focused them onto the detector D_2. The entrance aperture of the detector D_2 amounts to 30 mm, while the total path of the ion to the detector is 100 mm. The design of the electron optics was such that at least 95% of all the slow ions produced could be collected and recorded. The charge states of these ions were analyzed on the basis of the flight times of the ions to the detector D_2.

The pulses from detectors D_1 and D_2 were brought to the delayed-coincidence circuit CC and the coincidences were counted separately with the scaling circuit SC. To investigate the populations of the electronic states of the particles we measured the numbers of coincidences between fast and slow ions for specified scattering angles ϑ and appropriate specified kinetic-energy losses (or gains) ΔE by the fast particle. To monitor the stability of the gas density n_0 in the target chamber and the intensity I_0 of the primary ion beam we used the number N_2 of slow ions recorded by the detector D_2 and the scaling circuit SC_2, which is proportional to the product $n_0 I_0$.

The residual pressure in the chamber was 2×10^{-6} mm Hg, while the working pressure necessary to avoid excessive contamination by multiple collisions was $\gtrsim 1 \times 10^{-5}$ mm Hg. ³He was used as the working gas in the ion source and in the target chamber in order to be able to distinguish the He^{+2} ions from contaminating H_2^+ ions.

In one-electron capture,

$$He^{+2} + He \rightarrow He^+ + He^+ \tag{1}$$

FIG. 1. Experimental setup: I—ion source and beam forming system, M—magnetic mass analyzer, CA_1 to CA_5—collimating apertures, E_1—electrostatic deflection electrodes for displacing the beam parallel to itself, TC—target chamber, E_2—electrostatic deflection electrodes for extracting the slow ions produced in the gas from the chamber, E_3—electrodes for accelerating and focusing the slow ions, D_1, D_2, D_0—particle detectors, SC_1, SC_2, SC—scaling circuits, CC—coincidence circuits, A—electrostatic analyzer.

no free electrons are produced and the total kinetic-energy change ΔE of the colliding particles is determined by the change in the potential energy of the bound electrons as a result of the collision:

$$\Delta E = T_0 - T_1 - T_2 = I[He(1s^2)] - I_1[He^+(n_1)] - I_2[He^+(n_2)].$$

where T_0, T_1, and T_2 are the kinetic energies of the primary particle, the fast scattered particle, and the recoil particle, respectively; I, I_1, and I_2 are the total binding energies of the electrons in the target atom, the fast scattered particle, and the recoil particle, respectively; and n_1 and n_2 are the principal quantum numbers of the He$^+$ states. T_1 is determined directly with the aid of the analyzer A, while T_2 is determined from the relation $T_2 = T_0 \sin^2 \vartheta$, where ϑ is the fast-particle scattering angle, since the kinetic-energy change ΔE has very little effect on T_2.

In the case of capture with ionization,

$$He^{+2} + He \rightarrow He^+ + He^{+1} + e^- \qquad (2)$$
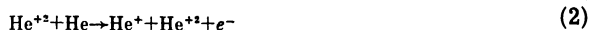
the change ΔE in the kinetic energy of the colliding particles is made up of the change in the potential energy of the bound electron and the kinetic energy T_e of the free electron:

$$\Delta E = T_0 - T_1 - T_2 = I[\text{He } (1s^2)] - I_1[\text{He}^+(n_1)] + T_e.$$

For a given electronic state He$^+(n_1)$, the observed spectrum of the inelastic energy losses by the fast particle corresponds to the kinetic-energy spectrum of the released electrons.

It should be noted that this method of measuring the energy spectra of the released electrons by analyzing the inelastic energy losses by the fast particle and its scattering angle with simultaneous determination of the charge and electronic states of both the scattered particle and the recoil particle has a number of advantages over the direct measurement of the kinetic energy of the electrons. Indeed, in this case one can distinguish the spectrum corresponding to a specific elementary process involving a change of the charge states and to the decay of a definite electronic state of the colliding particles. In addition, each electron spectrum corresponds to a definite impact parameter. Finally, one can investigate the shape of the spectrum down to values close to zero for the kinetic energy T_e of the released electrons.

III. EXPERIMENTAL RESULTS AND DISCUSSION

1. Passage to the quasimolecule, and capture process channels

In the range of colliding-particle velocities that we are interested in ($v = 0.16-0.9$ a.u.) the He^{+2} – He interaction can be treated in the quasimolecule approximation. Then one can use the adiabatic correlation diagram for the terms of the He$_2^{+2}$ system.[6] As the particles approach one another the term of the [He^0(1s^2) + He^{+2}] initial state splits into an even term, $(2p\sigma_u)^2$ $^1\Sigma_g^*$, which, in the limit in which the colliding particles are assumed to fuse to form a beryllium atom, gives the $2p^2$Be^{+2} state, and an odd term, $1s\sigma_g 2p\sigma_u {}^1\Sigma_u$, which gives the $1s2p$Be^{+2} state. The $^1\Sigma_g^*$ term (shown by a heavy curve in Fig. 2) runs close to the lowest $[(1s\sigma_g)^2 {}^1\Sigma_g]$ term of the [He$^+$(1s) + He$^+$(1s)] state in the region $R \sim 3-5$ a.u., while at $R \sim 1.5$ a.u. it crosses a term of the state [He$^+$(1s) + He$^+$(2s)]
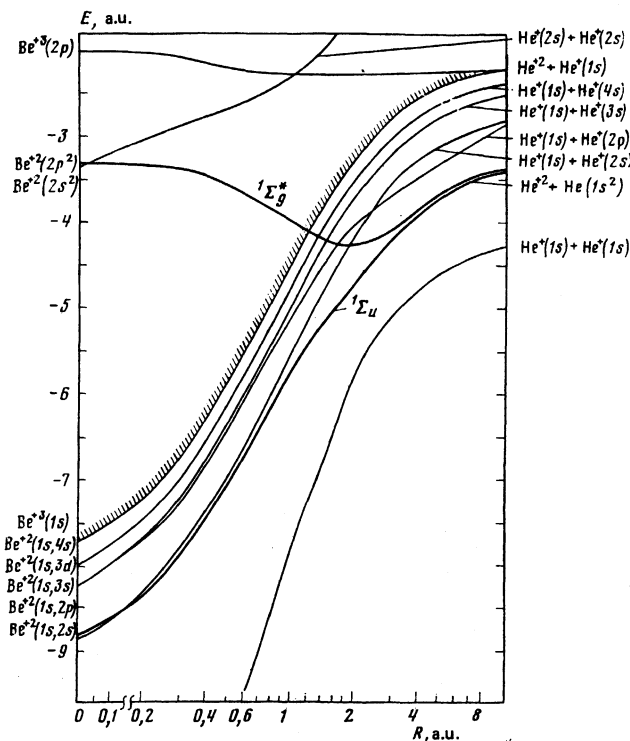

FIG. 2. Potential energy curves for Σ states of the He$_2^{+2}$ and He$_2^{+3}$ systems.[6] The heavy curves are for terms of the initial state, and the hatched curve is for [He$^+$(1s) + He^{+2}].

and then crosses a whole band of terms of the same symmetry belonging to the [He$^+$(1s) + He$^+$(n, l)] states. At low internuclear distances the initial $^1\Sigma_g^*$ term can interact with a term of a state that corresponds to the excitation of both ions—the [He$^+$(2s) + He$^+$(2s)] state. In addition, when $R < 1$ a.u. the $^1\Sigma_g^*$ term lies above the ionization energy of the He$_2^{+2}$ system (the [He^{+2} + He$^+$ (1s)] state, which is marked by a hatched curve on Fig. 2). Under these conditions the quasimolecule being formed can decay by an Auger transition, resulting in a process of capture with ionization or in a one-electron ionization process. Under these conditions the released electron should have the higher energy, the closer together the colliding particles were when the Auger transition took place.

At small internuclear distances the odd term of the initial state (the $1s\sigma_g 2p\sigma_u {}^1\Sigma_u$ term) comes close only to the $^3\Sigma_u$ term of the [He$^+$(1s) + He$^+$(1s)] state (not shown on Fig. 2), which has a different multiplicity, and to a term of the [He$^+$(1s) + He$^+$(2s)] state, which has the opposite parity. At low collision velocities, therefore, the odd term of the initial state can hardly interact with these terms at all, and the probability for the one-electron capture process should be determined by the interaction of the $^1\Sigma_g^*$ term. This conclusion is confirmed by experimental data on the differential cross sections for scattering of He$^+$ ions produced in the capture process (Fig. 4; see Part 3 of this Section).

It is evident from Fig. 3 that the main contribution to the capture process comes from the channels
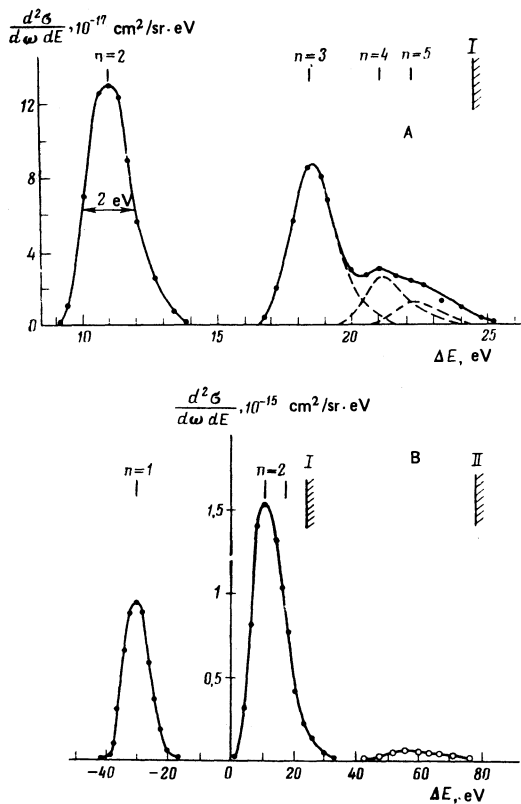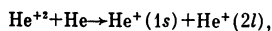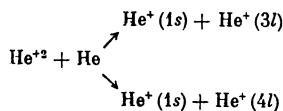
FIG. 3. Inelastic-energy-loss spectra for the fast particle in the one-electron capture process $He^{+2} + He \rightarrow He^+(1s) + He^+(n,l)$: A) $T_0 = 4.3$ keV, $\vartheta = 50'$; B) $T_0 = 30$ keV, $\vartheta = 0$. The principal quantum number of the excited state of one of the He^+ ions is denoted by n. The open circles represent points on the part of the spectrum corresponding to excitation of both ions.

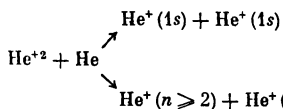$$He^{+2} + He \rightarrow He^+(1s) + He^+(2l), \qquad (a)$$

which lead to the formation of one He^+ ion in the ground (1s) state and the other in an excited (2s or 2p) state. Figure 3 also shows that the populations of the excited states of the He^+ ions decrease as the principal quantum number n increases beyond 2, the contributions from the channels

$$He^{+2} + He \begin{array}{c} \nearrow He^+(1s) + He^+(3l) \\ \\ \searrow He^+(1s) + He^+(4l) \end{array} \qquad \begin{array}{c} (b) \\ \\ (c) \end{array}$$

being quite small.

On comparing Figs. 3, A and 3, B, we see that the contributions from the channels

$$He^{+2} + He \begin{array}{c} \nearrow He^+(1s) + He^+(1s) \\ \\ \searrow He^+(n > 2) + He^+(n > 2), \end{array} \qquad \begin{array}{c} (d) \\ \\ (e) \end{array}$$

which lead to the formation of both ions in the ground state [channel (d)] or both in excited states [channel (e)], increase with increasing collision energy T_0. The contributions to the total capture cross section from chan-

nels (d) and (e) are 0.4% and 2%, respectively, at $T_0 = 4.3$ keV, and 25% and 4%, respectively, at $T_0 = 30$ keV.

The fact that channel (d) plays such a small part is due to the large energy separation between the $^1\Sigma_g^*$ term of the initial state $[He^{+2} + He^0]$ and a term of the $[He^+(1s) + He^+(1s)]$ state, while the contribution from channel (e) is small because this channel can become effective only at small internuclear distances.

2. Scattering incident to electron capture and the interaction region for quasimolecular terms

The internuclear distances at which the observed capture channels become operative can be estimated from particle-scattering data (Fig. 4). It will be seen that the lowest scattering angles (1.5 keV·deg) are associated with channel (d), in which both He^+ ions are produced in the ground state. On the basis of the terms for the states $^1\Sigma_g^*$ $[He^{+2} + He(1s^2)]$ and $[He^+(1s) + He^+(1s)]$ between which the electron transition takes place when electron capture occurs via channel (d) one can calculate the distance between the particles corresponding to the experimental scattering angle ~1.5 keV·deg. The distance found in this way turns out to be ~3 a.u. and corresponds to the internuclear distances at which these
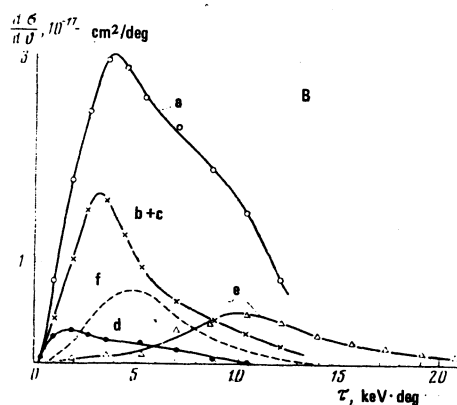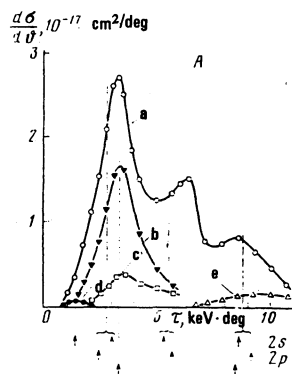

FIG. 4. Differential cross sections for scattering of fast He^+ ions at $T_0 = 4.3$ keV (A) and $T_0 = 10.4$ keV (B). The letters a–e mark the curves for the corresponding channels (a)–(e) of process (1) as defined in the text; the letter f marks the curve for process (2). The arrows below the abscissa axis of plot A mark the calculated positions of the peaks for electron capture into the 2s, 2p, and 3s states of the He^+ ion.

terms actually come closest together in energy. The two terms approach one another as R decreases from infinity to ~2 a.u.; this leads to partial cancelling of the repulsive forces between the nuclei and to weak scattering of the He⁺ ions in the one-electron capture channel (d).

The peaks of curves a, b, and c on Fig. 4, which correspond to channels in which one of the ions is produced in the ground state and the other in an excited state, lie in the reduced-angle range 3–3.5 keV·deg. Such scattering of the fast He⁺ ion corresponds to internuclear distances of ~1.5 a.u. and is associated with the crossing of a whole band of terms of $[He^+(1s) + He^+(n \gtrsim 2)]$ states by the $^1\Sigma_g^*$ initial-state term (Fig. 2).

The observed scattering confirms the virtual absence of transitions between the $^1\Sigma_u$ odd entrance-channel term and a term of the $[He^+(1s) + He^+(2s)]$ state. Indeed, on calculating the impact parameter using the interaction between the particles given by these terms one finds that the angle at which the differential scattering cross section is maximum (3.5 keV·deg) would correspond to a small impact parameter (0.4 a.u.) and therefore to a small cross section (3×10^{-18} cm²), which is ~20 times smaller than the experimental values (see curve a on Fig. 6).

The presence of structure in the angular distribution for channel (a) is striking. This structure is very evident at $T_0 = 4.3$ keV (Fig. 4, A) and somewhat smoothed out at $T_0 = 10.4$ keV (Fig. 4, B) because of the finite resolution (~20′) of the fast-particle collimator. The structure may be due to interference between scattering components associated with the development of the system along two different terms (along $^1\Sigma_g^*$ $[He^{+2} + He(1s^2)]$ and $[He^+(1s) + He^+(2s)]$ or $[He^+(1s) + He^+(2p)]$) in the region of internuclear distances R smaller than 1.5 a.u., which corresponds to the quasi-intersection of the terms and to the transition in channel (a). The terms of the He_2^{+2} system were used to estimate the impact parameters corresponding to the angles at which the differential scattering cross section has its maxima (the results were $R_1 = 0.95$, $R_2 = 0.65$, and $R_3 = 0.51$ a.u.), and then the scattering-amplitude phase differences for the development of the He_2^{+2} system according to two different terms (the initial $^1\Sigma_g^*$ term and the final $[He^+(1s) + He^+(2s)]$ or $[He^+(1s) + He^+(2p)]$ term) were calculated for these impact parameters.

The arrows on Fig. 4, A mark the scattering angles at which the scattering-amplitude phase differences for capture of the electron in the $2s$, $2p$, and $3s$ states of the He⁺ ion are integral multiples of 2π. It will be seen that the experimental values of the scattering angles at which the differential cross sections reach their maxima agree within 15–20% with these calculated values, thus confirming our assumption concerning the nature of the structure. The calculation also enables us to understand why the differential scattering cross sections for capture of the electron into more highly excited levels with $n \gtrsim 3$ (curve $b + c$ on Fig. 4, B) exhibit no analogous structure. In these cases the scattering-amplitude phase difference that leads to interference peaks should be reached at smaller impact parameters, and as a con-
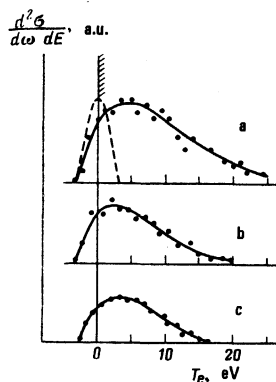

FIG. 5. Kinetic energy distributions of electrons produced in process (2) (capture with ionization) at $T_0 = 7.36$ keV: a) $\vartheta = 30'$, b) $\vartheta = 10'$, c) $\vartheta = 0$. The dashed curve represents the instrumental line shape.

sequence the second maxima on curves b and c should occur at scattering angles greater than 8.5 keV·deg and should not be high.

The differential cross section for the scattering that takes place when the reaction goes via channel (e), in which both He⁺ ions are produced in excited states, has its maximum in the region $\tau = T_0 \sim 8$–9 keV·deg, and this corresponds to a very small internuclear distance. This agrees well with the assumption that the corresponding transition takes place when the initial $^1\Sigma_g^*$ term crosses a term of the $[He^+(2s) + He^+(2s)]$ state at small internuclear distances.

When process (2)—capture with ionization—takes place the differential cross section for the scattering of the He⁺(1s) ions has its maximum at ~5 keV·deg (curve f on Fig. 4, B). Thus, this process takes place at shorter internuclear distances than the distance (corresponding to $\tau = 4$ keV·deg) at which the initial term enters the continuum of the He_2^{+2} system. As was noted above, the distribution of the energy losses of the fast particle in the capture-with-ionization process corresponds to the energy distribution of the electrons released in that process. Such electron energy distributions for various fast-ion scattering angles are shown in Fig. 5. It will be seen that the high-energy tail of the distribution becomes longer as the impact parameter decreases (as the scattering angle increases). This agrees well with the model according to which the capture-with-ionization process takes place via Auger decay of the excited quasimolecular system at various internuclear distances.

3. Absolute channel cross sections for the capture process and excited-state populations

From particle-scattering data for all the channels, summed over all impact parameters, one can derive the absolute cross sections for the capture process with formation of the ions in definite states (Fig. 6). The cross section for channel (d), in which both ions are produced in the 1s ground state, increases with increasing T_0 over the entire range (curve d on Fig. 6). The curve reaches no maximum in the investigated energy range;
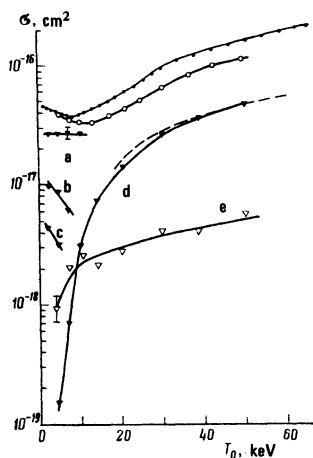
FIG. 6. T_0 dependences of the cross sections for various channels for process (1) (one-electron capture): ●—total one-electron capture cross section from Ref. 4; ∇—various channels for the $He^+ + He \rightarrow He^+(1s) + He^+(n,l)$ process (the letters a–d mark the curves for channels (a)–(d) as defined in the text: (a) —$n = 2$, (b) —$n = 3$, (c)—$n = 4$, (d)—$n = 1$; the dashed curve represents a theoretical calculation[7] for channel (d)); ∇—channel (e) $(He^{+2} + He \rightarrow He^+(n \geq 2) + He^+(n \geq 2))$; ○—total cross section for channels (a), (b), and (c).

this is apparently associated with the large energy gap (~25 eV) between the $^1\Sigma_g^*$ term of the initial state and the $[He^+ (1s) + He^+(1s)]$ final state in the region where these terms are closest together and with the fact that these terms run nearly parallel in that region.

Calculations of the cross section for this channel by the impact parameter method[7] led to good agreement with experimental data. The authors of Ref. 7 used wave functions for only three states, $[He^{+2} + He^0(1s^2)]$, $[He^0(1s^2) + He^{+2}]$, and $[He^+(1s) + He^+(1s)]$, in describing the He_2^{+2} system, the $[He^+(1s) + He^+(n \geq 2)]$ states being neglected, although according to our experimental data it is the transition probabilities to these states that are the highest. The fact that the calculation nevertheless leads to good agreement with experiment indicates that channels (a)–(c) have little effect on the cross section for channel (d), and this can be attributed to the fact that channels (a)–(c) are populated at much shorter internuclear distances ($R \sim 1.5$ a.u.) than those at which process (d) takes place (3–5 a.u.). As a result, the impact-parameter region that makes the main contribution to the channel-(d) cross section lies outside the region in

which the transitions involved in channels (a)–(c) take place.

The cross sections for channels (b) and (c), which involve the formation of one of the He^+ ions in a $3l$ or $4l$ state, decrease rapidly with increasing collision energy T_0. This behavior, together with the fact that the cross sections for channels (a) and (d) exhibit the opposite behavior (the cross sections increase with increasing T_0), results in the total cross section having a minimum as a function of T_0.

Thus, the quasimolecular interaction picture gives a good account of the He^{+2} – He collision in the 2–60 keV energy range. The experiment has shown that the channel in which one of the ions is left after the collision in an excited state plays the main part in the one-electron capture process. The capture channel in which both the ions are left in the $He^+(1s)$ ground state after the collision is effective only at high collision energies ($T_0 > 30$ keV). The contribution from the channel in which both ions are produced in excited states is insignificant. The one-electron-ionization and capture-with-ionization processes result from the decay of a self-ionization state of the He_2^{+2} quasimolecule formed in the collision.

In conclusion, the authors express their deep gratitude to O. B. Firsov for participating in a discussion of the results, and to V. K. Nikulin for valuable discussions.

[1] Z. Z. Latypov, I. F. Flaks, and A. A. Shaporenko, Zh. Eksp. Teor. Fiz. 57, 1987 (1969) [Sov. Phys.-JETP 30, 1076 (1970)].
[2] R. H. Berkner, R. V. Pyle, J. W. Sterns, and J. C Warren, Phys. Rev. 166, 44 (1968).
[3] M. W. Siegel, Y. H. Chen, and J. W. Boring, Phys. Rev. Lett. 28, 465 (1972); Y. H. Chen, R E. Johnson, R. R Humphris, and M. W. Siegel, J. Phys. B8, 1527 (1975).
[4] V. V. Afrosimov, G. A Leiko, Yu. A. Mamaev, and M. N. Panov, Abstracts of Papers, Eighth International Conference on the Physics of Electronic and Atomic Collisions, Beograd, Yugoslavia, 1973, p. 183; Zh. Eksp. Teor. Fiz. 67, 1329 (1974) [Sov. Phys.-JETP 40, 661 (1974)].
[5] V. V. Afrosimov, G. A. Leiko, and M. N. Panov, Abstracts of Papers, Ninth International Conference on the Physics of Electronic and Atomic Collisions, Seattle, Wash., USA, 1975, p. 183.
[6] V. K. Nikulin and N. A. Gushchina, Zh. Tekh. Fiz. 48, 13 (1978) [Sov. Phys. Tech. Phys. 23, 7 (1978)].
[7] Margaret J. Fulton and M. H. Mittleman, Proc. Phys. Soc. 87, 669 (1966).

Translated by E. Brunner